Fixed-Time Command-Filtered Adaptive Backstepping Control for a Class of Uncertain MIMO Systems

Xianlei Zhang, Yan Zhang, Qing Hu, Anjie Yang, Xuan Li

College of Artificial Intelligence and Data Science,
Hebei University of Technology, Tianjin, 300401, China
(e-mail: hbgyzxl@163.com, yzhangz@163.com).

Abstract: This paper studies the fixed-time tracking control for multi-input multi-output (MIMO) nonlinear systems with uncertainties and external disturbances. Based on command-filtered technique, an adaptive fixed-time backstepping control method is proposed. Compared with the existing finite-time control, the settling time does not depend on initial conditions. The prediction error generated by the serial-parallel estimation model is combined with error compensation signal to construct a network adaptive law for weight updating. Meanwhile, the external disturbance and network approximation error compose lumped disturbance, which is estimated by the adaptive disturbance observer. Through strict theoretical analysis, the tracking error converges to a small neighborhood of the origin within a fixed time and all signals in the control system are bounded. Two simulation examples are given to demonstrate the benefits of the presented method.

Keywords: Fixed-time control (FiTC), command-filtered, backstepping, serial-parallel estimation model (SPEM), neural networks.

1. INTRODUCTION

In recent years, the adaptive backstepping method has been utilized in real-time tracking control owing to its recursive design framework (Ata and Coban, 2022; Van et al., 2019; Vallejo Alarcon, 2020). Nonetheless, the virtual controller needs to be differentiated repeatedly for the classical backstepping technique, which leads to a significant increase in computational complexity. To avoid this problem, the dynamic surface control scheme was investigated by letting the virtual controller pass through filter to replace complicated differential operation (Swaroop et al., 2000; Shojaei et al., 2019; Liu et al., 2020; Ma et al., 2019). Additionally, (Farrell et al., 2009 and Dong et al., 2012) developed command-filtered backstepping (CFB) approach to avoid repeated differentiation and eliminate filtering error simultaneously.

For uncertain nonlinear control systems with external disturbances, fuzzy logic systems and neural networks (NNs) have been mainly used to approximate unknown nonlinear functions because of their universal approximation abilities (Euldji et al., 2022; Chen and Lin, 2021; Van Tran and Wang, 2017; Wang et al., 2018a; Dong et al., 2022; Jebri et al., 2020). Especially, NNs have been extensively employed in a variety of backstepping control schemes (Zhang et al., 2018; Yu et al., 2020; Niu et al., 2017; Qiu et al., 2020; Cao et al., 2018; Chen et al., 2010). The approximation precision of NN has a large influence on system performance. Fortunately, the approximation capacity of NN can be assessed by prediction error derived from serial-parallel estimation model (SPEM). Some promising researches have been carried out (Xu et al., 2020; Xu and Sun, 2018; Sun et al., 2020; Xu, 2018), which constructed network adaptive laws (NALs) with prediction errors to improve approximation precisions. At the same time, (Wang et al., 2018b and Li et al., 2015) developed SPEM-based adaptive fuzzy control approaches to increase approximation abilities. Nevertheless, the aforesaid methods can only assure asymptotic stability. In other words, the error convergence is realized as time goes to infinity.

Compared with asymptotic control schemes, the finite-time control (FTC) guarantees that the control objective can be achieved in a limited time. (Sun et al., 2022) presented a finite-time composite adaptive neural control (FTCANC) method to achieve high-precision tracking performance. (Yu et al., 2018) proposed a finite-time command-filtered backstepping control method to solve the problem of finite-time tracking control for a class of high-order nonlinear systems. However, the upper bound of settling time (UBOST) of FTC relies on initial conditions. The settling time will become unacceptable when initial conditions are far from the origin. Fortunately, (Polyakov, 2012) proposed a fixed-time control (FiTC) strategy to resolve this problem. This method has all advantages of FTC and the UBOST is only determined by control parameters. In the meantime, many academics have employed FiTC to deal with tracking problems (Ba et al., 2019; Sun et al., 2023; Yang and Ye, 2018; Guo et al., 2022; Yang et al., 2021; Kanchanaharuthai and Mujjalinvimut, 2022; Gao and Guo, 2019; Song et al., 2021). For example, a fixed-time adaptive neural control (FiTANC) method was investigated in (Ba et al., 2019) to address the fixed-time adaptive control for nonstrict feedback nonlinear systems. (Sun et al., 2023) proposed a fixed-time adaptive control scheme to improve the control performance for nonlinear systems subject to input saturations. (Yang et al., 2021) put

* This article was supported by National Natural Science Foundation of China (Grant 61773151), National Key R & D Program (Grant 2020YFC2007702).
* Corresponding author, Yan Zhang.

forward an observer-based adaptive fixed-time control strategy for constrained nonstrict feedback nonlinear systems with prescribed performance. Although FiTC methods have achieved a series of superior results, there still exist a issue to be settled. The constructed NALs are only yielded by tracking errors, which cannot assure accurate approximation.

Based on above analysis, this paper proposes a command-filtered based fixed-time adaptive backstepping control approach to achieve high-precision trajectory tracking. The radial basis function NNs (RBFNNs) are employed to approximate uncertainties. The NALs containing error compensation signals and prediction errors are constructed for weights updating to improve the approximation precision. The adaptive disturbance observers (ADOs) are designed to estimate lumped disturbances fused by external disturbances and approximation errors of RBFNNs.

Compared with previous results, the main innovations of this paper can be stated as follows.

1) Different from previous FiTC schemes (Ba et al., 2019; Sun et al., 2023; Yang and Ye, 2018; Guo et al., 2022; Yang et al., 2021; Kanchanaharuthai and Mujjalinvimut, 2022; Gao and Guo, 2019; Song et al., 2021), the NALs are constructed by error compensation signals and prediction errors, which can improve the approximation precision. New virtual controllers and error compensation signals are designed to guarantee the system is fixed-time stable.
2) Compared with existing composite control (Xu et al., 2020; Xu and Sun, 2018; Sun et al., 2020; Xu, 2018; Wang et al., 2018b; Li et al., 2015; Sun et al., 2022), this paper presents a novel SPEM to generate prediction error, which contributes to the fixed-time stability of control plant. The approximation accuracy of NN is improved under NALs.
3) Unlike conventional disturbance observers (Kanchanaharuthai and Mujjalinvimut, 2022; Gao and Guo, 2019; Song et al., 2021), the developed ADOs can estimate lumped disturbances synthesized by external disturbances and approximation errors of NNs. The control performance can be greatly enhanced by using ADOs for disturbance compensation.

The rest of this paper is organized as follows. Section 2 shows the system information. Section 3 reveals the specific controller design and stability analysis. Two simulation examples are given in Section 4 to verify the validity of the investigated method, and Section 5 presents the conclusion.

2. PROBLEM FORMULATION AND PRELIMINARIES

2.1 Preliminaries

Definition 1 (Sun et al., 2023). Consider the following nonlinear system:

$$\dot{x}(t)=f(x(t)),\ f(0)=0,\ x(0)=x_0 \tag{1}$$

where $f:\mathbb{R}_+\times\mathbb{R}^n\to\mathbb{R}^n$ is a nonlinear function, $x(t)\in\mathbb{R}^n$ represents the system state signal. The system (1) is practically fixed-time stable (FiTS) if there exist constants $\delta>0$, $T_{\max}>0$ and a bounded settling time $T(\delta,x_0)\le T_{\max}$ such that $\|x(t)\|<\delta$ holds for $\forall t>T(\delta,x_0)$.

Lemma 1 (Ba et al., 2019). For system (1), if there is a positive-define Lyapunov function $V(x)$ satisfying

$$\dot{V}(x)\le -p_1V^{\lambda_1}(x)-p_2V^{\lambda_2}(x)+c$$

where the constants $p_1,p_2>0$, $\lambda_1>1$, $0<\lambda_2<1$ and scalar $0<c<\infty$. Then the system (1) is practically FiTS and the settling time T can be expressed as

$$T\le T_{\max}=\frac{1}{p_1\bar{\varsigma}(\lambda_1-1)}+\frac{1}{p_2\bar{\varsigma}(1-\lambda_2)}$$

The residual set of the solution of system (1) is given by

$$x\in\left\{V(x)\le\min\left\{\left(\frac{c}{(1-\bar{\varsigma})p_1}\right)^{\frac{1}{\lambda_1}},\left(\frac{c}{(1-\bar{\varsigma})p_2}\right)^{\frac{1}{\lambda_2}}\right\}\right\}$$

where $0<\bar{\varsigma}<1$.

Lemma 2 (Zuo and Tie, 2014). For constant $p>0$ and variable $x_j\in\mathbb{R}$ $(j=1,2,...,n)$, one obtains

$$\begin{cases}\left(\sum_{j=1}^{n}|x_j|\right)^p\le\sum_{j=1}^{n}|x_j|^p, & 0<p\le 1\\ n^{1-p}\left(\sum_{j=1}^{n}|x_j|\right)^p\le\sum_{j=1}^{n}|x_j|^p, & p>1\end{cases}$$

Lemma 3 (Qian and Lin, 2001). For any given positive numbers h_1, h_2 and real-valued function $s(x,y)>0$, the following holds for $\forall x,y\in\mathbb{R}$.

$$|x|^{h_1}|y|^{h_2}\le\frac{h_1}{h_1+h_2}s(x,y)|x|^{h_1+h_2}+\frac{h_2}{h_1+h_2}s^{-\frac{h_1}{h_2}}(x,y)|y|^{h_1+h_2}$$

Lemma 4 (Yu et al., 2020). If $H_{i,j}(Z_{i,j})$ is a continuous function defined on a compact set $\Omega_{i,j}$, there exists an RBFNN $W_{i,j}^TS_{i,j}(Z_{i,j})$ such that

$$H_{i,j}(Z_{i,j})=W_{i,j}^TS_{i,j}(Z_{i,j})+\delta_{i,j}$$

where $Z_{i,j}=[Z_{i,j,1},Z_{i,j,2},...,Z_{i,j,\bar{r}}]^T\in\mathbb{R}^{\bar{r}}$ represents the network input with $\bar{r}$ nodes. $W_{i,j}=[W_{i,j,1},W_{i,j,2},...,W_{i,j,l}]^T\in\mathbb{R}^l$ indicates the network weight with l codes. $\delta_{i,j}$ is the approximation error, satisfying $|\delta_{i,j}|\le\bar{\delta}_{i,j,1}$ and $|\dot{\delta}_{i,j}|\le\bar{\delta}_{i,j,2}$. $\bar{\delta}_{i,j,1}$ and $\bar{\delta}_{i,j,2}$ are unknown positive numbers. $S_{i,j}(Z_{i,j})=[s_{i,j,1},s_{i,j,2},...,s_{i,j,l}]^T\in\mathbb{R}^l$ is the network basis function, $s_{i,j,\kappa}$ is the Gaussian function defined as

$$s_{i,j,\kappa}=\exp\left(-\frac{\|Z_{i,j}-c_{i,j}\|^2}{2b_\kappa^2}\right)$$

where $c_{i,j}=[c_{i,j,1},c_{i,j,2},...,c_{i,j,\bar{r}}]^T\in\mathbb{R}^{\bar{r}}$ is the center vector and b_κ is the width parameter, $\kappa=1,2,...,l$.

2.2 Problem formulation

Consider the following uncertain MIMO nonlinear system:

$$\begin{cases}\dot{x}_{i,j}=f_{i,j}(\bar{x}_{i,j})+g_{i,j}(\bar{x}_{i,j})x_{i,j+1}+d_{i,j}(t)\\ \dot{x}_{i,n_i}=f_{i,n_i}(\bar{x}_{i,n_i})+g_{i,n_i}(\bar{x}_{i,n_i})u_i+d_{i,n_i}(t)\\ y_i=x_{i,1}\end{cases}\tag{2}$$

where $i=1,2,...,n$ and $j=1,2,...,n_i-1$. In the ith subsystem, $\bar{x}_{i,j}=[x_{i,1},x_{i,2},...,x_{i,j}]^T\in\mathbb{R}^j$ denotes the state vector of the jth differential equation. $f_{i,j}(\bullet)$ represents the unknown nonlinear function. $g_{i,j}(\bullet)$ is the known bounded function. $d_{i,j}(\bullet)$ stands for the external disturbance. u_i and y_i are the input and output respectively.

Assumption 1 (Wang et al., 2018b). Desired signals $y_{i,d}$ and $\dot{y}_{i,d}$ are known smooth bounded functions.

Assumption 2 (Zhao and Song, 2019). There exist positive numbers $\bar{g}_1$ and $\bar{g}_2$ such that $\bar{g}_1\le|g_{i,j}(\bullet)|\le\bar{g}_2$ holds.

Assumption 3 (Xu and Sun, 2018). There exist positive numbers $\bar{d}_{i,j,1}$ and $\bar{d}_{i,j,2}$ such that $|d_{i,j}(t)|\le\bar{d}_{i,j,1}$ and $|\dot{d}_{i,j}(t)|\le\bar{d}_{i,j,2}$ hold.

Remark 1. Assumption 1 is commonly utilized in tracking control. Assumption 2 represents that the control gain $g_{i,j}(\bullet)$ in (2) is a nonzero bounded function, revealing the controllability of the control system. The constants $\bar{g}_1$ and $\bar{g}_2$ are only employed for the stability analysis, whose specific values are not need to be known. Assumption 3 is generically used in disturbance observer design.

The control target of this paper is to design a fixed-time command-filtered backstepping controller. The tracking error converges to a small neighborhood of the origin within a fixed time and all signals of the control plant are bounded.

To simplify analysis, $f_{i,j}(\bar{x}_{i,j})$, $g_{i,j}(\bar{x}_{i,j})$, $d_{i,j}(t)$ and $S_{i,j}(Z_{i,j})$ are abbreviated as $f_{i,j}$, $g_{i,j}$, $d_{i,j}$ and $S_{i,j}$ respectively.

3. CONTROLLER DESIGN AND STABILITY ANALYSIS

3.1 Design the fixed-time backstepping controller

The tracking errors are designed as

$$\begin{cases}z_{i,1}=y_i-y_{i,d}\\ z_{i,j}=x_{i,j}-x_{i,j}^c\end{cases}\tag{3}$$

where $y_{i,d}$ represents the desired signal, $x_{i,j}^c$ represents the output signal of the filter, $i=1,2,...,n$, $j=2,...,n_i$. The filter is introduced as follows (Gao and Guo, 2019):

$$\begin{aligned}&\dot{\varphi}_{i,j,1}=\beta_{i,j,1}\\ &\beta_{i,j,1}=-k_{i,j,1}\left|\Psi_{i,j}\right|^{l_{i,j,1}}sign\left(\Psi_{i,j}\right)\\ &\quad-k_{i,j,2}\left|\Psi_{i,j}\right|^{l_{i,j,2}}sign\left(\Psi_{i,j}\right)+\varphi_{i,j,2}\\ &\dot{\varphi}_{i,j,2}=-k_{i,j,3}\left|\Psi_{i,j}\right|^{l_{i,j,3}}sign\left(\Psi_{i,j}\right)\\ &\quad-k_{i,j,4}\left|\Psi_{i,j}\right|^{l_{i,j,4}}sign\left(\Psi_{i,j}\right)\end{aligned}\tag{4}$$

where $\Psi_{i,j}=\varphi_{i,j,1}-\alpha_{i,j}$ is the filtering error satisfying $\left|\Psi_{i,j}\right|\le\Sigma_j$, the virtual controller $\alpha_{i,j}$ is the input signal, $x_{i,j}^c=\varphi_{i,j,1}$ is the output signal, $\dot{x}_{i,j}^c=\beta_{i,j,1}$. $k_{i,j,s}>0$ ($s=1,2,3,4$) are design parameters, $0<l_{i,j,1},l_{i,j,3}<1$ and $l_{i,j,2},l_{i,j,4}>1$ are constants.

In order to eliminate $\Psi_{i,j}$, the filtering error compensation signal (FECS) and tracking error compensation signal (TECS) are defined as $\eta_{i,j}$ and $v_{i,j}$, respectively. The following is satisfied.

$$v_{i,j}=z_{i,j}-\eta_{i,j}\tag{5}$$

The virtual controllers are designed as

$$\alpha_{i,1}=\frac{1}{g_{i,1}}\begin{bmatrix}-\frac{l_{i,1}}{2}v_{i,1}-h_{i,1}\left|v_{i,1}\right|^{\gamma_2}sign(v_{i,1})\\ -p_{i,1}v_{i,1}^{\gamma_1}-\hat{W}_{i,1}^TS_{i,1}-\hat{\varepsilon}_{i,1}+\dot{y}_{i,d}\end{bmatrix}\tag{6}$$

$$\alpha_{i,j}=\frac{1}{g_{i,j}}\begin{bmatrix}-\frac{l_{i,j}}{2}v_{i,j}-p_{i,j}v_{i,j}^{\gamma_1}-h_{i,j}\left|v_{i,j}\right|^{\gamma_2}sign(v_{i,j})\\ -g_{i,j-1}z_{i,j-1}-\hat{W}_{i,j}^TS_{i,j}-\hat{\varepsilon}_{i,j}+\dot{x}_{i,j}^c\end{bmatrix}\tag{7}$$

where $p_{i,j}>0$, $h_{i,j}>0$, $l_{i,j}>0$, $\gamma_1>1$ and $0<\gamma_2<1$ are constants. $\hat{\varepsilon}_{i,j}$ and $\hat{W}_{i,j}$ are estimations of $\varepsilon_{i,j}$ and $W_{i,j}$, respectively. $\varepsilon_{i,j}$ is the lumped disturbance and will be defined later.

The FECSs are constructed as

$$\begin{aligned}\dot{\eta}_{i,1}=&-s_{i,1}\eta_{i,1}^{\gamma_1}-r_{i,1}\left|\eta_{i,1}\right|^{\gamma_2}sign(\eta_{i,1})\\ &+g_{i,1}\Psi_{i,1}+g_{i,1}\eta_{i,2}-l_{i,1}sign(\eta_{i,1})\end{aligned}\tag{8}$$

$$\begin{aligned}\dot{\eta}_{i,j}=&-s_{i,j}\eta_{i,j}^{\gamma_1}-r_{i,j}\left|\eta_{i,j}\right|^{\gamma_2}sign(\eta_{i,j})+g_{i,j}\Psi_{i,j}\\ &+g_{i,j}\eta_{i,j+1}-g_{i,j-1}\eta_{i,j-1}-l_{i,j}sign(\eta_{i,j})\end{aligned}\tag{9}$$

$$\begin{aligned}\dot{\eta}_{i,n_i}=&-s_{i,n_i}\eta_{i,n_i}^{\gamma_1}-r_{i,n_i}\left|\eta_{i,n_i}\right|^{\gamma_2}sign(\eta_{i,n_i})\\ &-g_{i,j-1}\eta_{i,j-1}-l_{i,n_i}sign(\eta_{i,n_i})\end{aligned}\tag{10}$$

where the constants $s_{i,j}>0$ and $r_{i,j}>0$.

To improve approximation capacity of NN, the prediction error is defined as $x_{z,i,j}=x_{i,j}-\hat{x}_{i,j}$, where $\hat{x}_{i,j}$ is deduced from the following SPEM:

$$\begin{cases}\dot{\hat{x}}_{i,j}=\hat{W}_{i,j}^TS_{i,j}+\hat{\varepsilon}_{i,j}+g_{i,j}x_{i,j+1}\\ \qquad+\rho_{i,j,1}x_{z,i,j}^{\gamma_1}+\rho_{i,j,2}\left|x_{z,i,j}\right|^{\gamma_2}sign(x_{z,i,j})\\ \dot{\hat{x}}_{i,n_i}=\hat{W}_{i,n_i}^TS_{i,n_i}+\hat{\varepsilon}_{i,n_i}+g_{i,n_i}u_i\\ \qquad+\rho_{i,n_i,1}x_{z,i,n_i}^{\gamma_1}+\rho_{i,n_i,2}\left|x_{z,i,n_i}\right|^{\gamma_2}sign(x_{z,i,n_i})\end{cases}\tag{11}$$

where $\rho_{i,j,1}$ and $\rho_{i,j,2}$ are positive numbers, $\hat{\varepsilon}_{i,n_i}$ and $\hat{W}_{i,n_i}$ are estimations of ε_{i,n_i} and W_{i,n_i}, respectively. ε_{i,n_i} is the lumped disturbance.

Remark 2. Unlike the prediction error built in previous composite adaptive control (Xu et al., 2020; Xu and Sun, 2018; Sun et al., 2020; Xu, 2018; Wang et al., 2018b; Li et al., 2015; Sun et al., 2022), the presented SPEM has fractional power terms $x_{z,i,j}^{\gamma_1}$ and $\left|x_{z,i,j}\right|^{\gamma_2} sign(x_{z,i,j})$, which contribute to the fixed-time stability of the control plant (2).

Thereby, through employing the prediction error $x_{z,i,j}$ and error compensation signal $v_{i,j}$, the NAL $\hat{W}_{i,j}$ is constructed as

$$\dot{\hat{W}}_{i,j} = a_{i,j,1}(v_{i,j} + a_{i,j,2}x_{z,i,j})S_{i,j} - \vartheta_{i,j}\hat{W}_{i,j} \tag{12}$$

where $a_{i,j,1} > 0$, $a_{i,j,2} > 0$ and $\vartheta_{i,j} > 0$ are constants.

The lumped disturbance $\varepsilon_{i,j}$ is estimated by following ADOs:

$$\begin{cases} \hat{\varepsilon}_{i,j} = L_{i,j}(x_{i,j} - \chi_{i,j}) \\ \dot{\chi}_{i,j} = \hat{W}_{i,j}^T S_{i,j} + \hat{\varepsilon}_{i,j} + g_{i,j}x_{i,j+1} - L_{i,j}^{-1}v_{i,j} \end{cases} \tag{13}$$

$$\begin{cases} \hat{\varepsilon}_{i,n_i} = L_{i,n_i}(x_{i,n_i} - \chi_{i,n_i}) \\ \dot{\chi}_{i,n_i} = \hat{W}_{i,n_i}^T S_{i,n_i} + \hat{\varepsilon}_{i,n_i} + g_{i,n_i}u_i - L_{i,n_i}^{-1}v_{i,n_i} \end{cases} \tag{14}$$

where $L_{i,j}$ is a positive number and $\chi_{i,j}$ is the internal state.

The practical control signal is designed as

$$u_i = \frac{1}{g_{i,n_i}}\begin{bmatrix} -\dfrac{l_{i,n_i}}{2}v_{i,n_i} - p_{i,n_i}v_{i,n_i}^{\gamma_1} - h_{i,n_i}\left|v_{i,n_i}\right|^{\gamma_2} sign(v_{i,n_i}) \\ -g_{i,n_i-1}z_{i,n_i-1} - \hat{W}_{i,n_i}^T S_{i,n_i} - \hat{\varepsilon}_{i,n_i} + \dot{x}_{i,n_i}^c \end{bmatrix} \tag{15}$$

where the constants $p_{i,n_i} > 0$, $h_{i,n_i} > 0$ and $l_{i,n_i} > 0$, $i = 1,2,...,n$.

3.2 Stability analysis

The following theorem states the main result of this paper.

Theorem 1. Consider the uncertain MIMO system (2) under Assumptions 1-3, applying the virtual controllers (6),(7), the FECSs (8)-(10), the SPEM (11), the NAL (12), the ADOs (13),(14) and the controller (15). The tracking performance can be achieved in a fixed time and all signals of the closed-loop system are bounded.

Proof. The backstepping-based specific analysis processes are as follows.

Step i,1 $(1 \le i \le n)$:

Based on (2) and (3), $\dot{x}_{i,1}$ can be rewritten as

$$\dot{x}_{i,1} = g_{i,1}z_{i,2} + g_{i,1}\alpha_{i,1} + g_{i,1}(x_{i,2}^c - \alpha_{i,1}) + W_{i,1}^T S_{i,1} + \varepsilon_{i,1} \tag{16}$$

where $f_{i,1} = W_{i,1}^T S_{i,1} + \delta_{i,1}$, $\varepsilon_{i,1} = d_{i,1} + \delta_{i,1}$ satisfies $\left|\varepsilon_{i,1}\right| \le \left|d_{i,1}\right| + \left|\delta_{i,1}\right| \le \zeta_{i,1,1}$ and $\left|\dot{\varepsilon}_{i,1}\right| \le \left|\dot{d}_{i,1}\right| + \left|\dot{\delta}_{i,1}\right| \le \zeta_{i,1,2}$, $\zeta_{i,1,1}$ and $\zeta_{i,1,2}$ are positive numbers.

With the help of (3), (6) and (16), the derivative of $z_{i,1}$ is calculated as

$$\begin{aligned} \dot{z}_{i,1} = &-\frac{l_{i,1}}{2}v_{i,1} - p_{i,1}v_{i,1}^{\gamma_1} - h_{i,1}\left|v_{i,1}\right|^{\gamma_2} sign(v_{i,1}) \\ &+ g_{i,1}\Psi_{i,1} + g_{i,1}z_{i,2} + \tilde{W}_{i,1}^T S_{i,1} + \tilde{\varepsilon}_{i,1} \end{aligned} \tag{17}$$

where $\tilde{W}_{i,1} = W_{i,1} - \hat{W}_{i,1}$ and $\tilde{\varepsilon}_{i,1} = \varepsilon_{i,1} - \hat{\varepsilon}_{i,1}$ are estimation errors.

Design the following Lyapunov function:

$$V_{i,1} = \frac{1}{2}v_{i,1}^2 + \frac{1}{2}\eta_{i,1}^2 + \frac{1}{2}a_{i,1,2}x_{z,i,1}^2 + \frac{1}{2a_{i,1,1}}\tilde{W}_{i,1}^T\tilde{W}_{i,1} + \frac{1}{2}\tilde{\varepsilon}_{i,1}^2 \tag{18}$$

According to (2), (8), (11)-(13) and (17), the derivative of $V_{i,1}$ is yielded as

$$\begin{aligned} \dot{V}_{i,1} = &-\frac{l_{i,1}}{2}v_{i,1}^2 - p_{i,1}v_{i,1}^{\gamma_1+1} - h_{i,1}\left|v_{i,1}\right|^{\gamma_2+1} - s_{i,1}\eta_{i,1}^{\gamma_1+1} - r_{i,1}\left|\eta_{i,1}\right|^{\gamma_2+1} \\ &- l_{i,1}\left|\eta_{i,1}\right| - \rho_{i,1,1}a_{i,1,2}x_{z,i,1}^{\gamma_1+1} - \rho_{i,1,2}a_{i,1,2}\left|x_{z,i,1}\right|^{\gamma_2+1} \\ &- L_{i,1}\tilde{\varepsilon}_{i,1}(\tilde{W}_{i,1}^T S_{i,1} + \tilde{\varepsilon}_{i,1}) + s_{i,1}v_{i,1}\eta_{i,1}^{\gamma_1} + r_{i,1}v_{i,1}\left|\eta_{i,1}\right|^{\gamma_2} sign(\eta_{i,1}) \\ &+ l_{i,1}v_{i,1}sign(\eta_{i,1}) + g_{i,1}\eta_{i,1}(x_{i,2}^c - \alpha_{i,1}) + g_{i,1}v_{i,1}v_{i,2} \\ &+ g_{i,1}\eta_{i,1}\eta_{i,2} + a_{i,1,2}x_{z,i,1}\tilde{\varepsilon}_{i,1} + \frac{\vartheta_{i,1}}{a_{i,1,1}}\tilde{W}_{i,1}^T\hat{W}_{i,1} + \tilde{\varepsilon}_{i,1}\dot{\varepsilon}_{i,1} \end{aligned} \tag{19}$$

Step i, j $(2 \le j \le n_i - 1, 1 \le i \le n)$:

By the virtue of (2) and (3), it can be deduced that

$$\dot{x}_{i,j} = g_{i,j}z_{i,j+1} + g_{i,j}\alpha_{i,j} + g_{i,j}(x_{i,j+1}^c - \alpha_{i,j}) + W_{i,j}^T S_{i,j} + \varepsilon_{i,j} \tag{20}$$

where $f_{i,j} = W_{i,j}^T S_{i,j} + \delta_{i,j}$, $\varepsilon_{i,j} = d_{i,j} + \delta_{i,j}$ satisfies $\left|\varepsilon_{i,j}\right| \le \left|d_{i,j}\right| + \left|\delta_{i,j}\right| \le \zeta_{i,j,1}$ and $\left|\dot{\varepsilon}_{i,j}\right| \le \left|\dot{d}_{i,j}\right| + \left|\dot{\delta}_{i,j}\right| \le \zeta_{i,j,2}$, the constants $\zeta_{i,j,1}, \zeta_{i,j,2} > 0$.

With the help of (3), (7) and (20), the derivative of $z_{i,j}$ is obtained as

$$\begin{aligned} \dot{z}_{i,j} = &-\frac{l_{i,j}}{2}v_{i,j} - p_{i,j}v_{i,j}^{\gamma_1} - h_{i,j}\left|v_{i,j}\right|^{\gamma_2} sign(v_{i,j}) + g_{i,j}(x_{i,j+1}^c - \alpha_{i,j}) \\ &+ g_{i,j}z_{i,j+1} - g_{i,j-1}z_{i,j-1} + \tilde{W}_{i,j}^T S_{i,j} + \tilde{\varepsilon}_{i,j} \end{aligned} \tag{21}$$

where $\tilde{W}_{i,j} = W_{i,j} - \hat{W}_{i,j}$ and $\tilde{\varepsilon}_{i,j} = \varepsilon_{i,j} - \hat{\varepsilon}_{i,j}$ are estimation errors.

The Lyapunov function is defined as

$$\begin{aligned} V_{i,j} = &\sum_{k=1}^{j-1} V_{i,k} + \frac{1}{2}v_{i,j}^2 + \frac{1}{2}\eta_{i,j}^2 + \frac{1}{2}a_{i,j,2}x_{z,i,j}^2 \\ &+ \frac{1}{2a_{i,j,1}}\tilde{W}_{i,j}^T\tilde{W}_{i,j} + \frac{1}{2}\tilde{\varepsilon}_{i,j}^2 \end{aligned} \tag{22}$$

According to (2), (9), (11)-(13) and (21), the derivative of $V_{i,j}$ is derived as

$$\begin{aligned} \dot{V}_{i,j} = &-\frac{1}{2}\sum_{k=1}^{j} l_{i,k}v_{i,k}^2 - \sum_{k=1}^{j} p_{i,k}v_{i,k}^{\gamma_1+1} - \sum_{k=1}^{j} h_{i,k}\left|v_{i,k}\right|^{\gamma_2+1} - \sum_{k=1}^{j} s_{i,k}\eta_{i,k}^{\gamma_1+1} \\ &- \sum_{k=1}^{j} r_{i,k}\left|\eta_{i,k}\right|^{\gamma_2+1} - \sum_{k=1}^{j} l_{i,k}\left|\eta_{i,k}\right| - \sum_{k=1}^{j} \rho_{i,k,1}a_{i,k,2}x_{z,i,k}^{\gamma_1+1} \\ &- \sum_{k=1}^{j} \rho_{i,k,2}a_{i,k,2}\left|x_{z,i,k}\right|^{\gamma_2+1} - \sum_{k=1}^{j} L_{i,k}\tilde{\varepsilon}_{i,k}(\tilde{W}_{i,k}^T S_{i,k} + \tilde{\varepsilon}_{i,k}) \\ &+ \sum_{k=1}^{j} s_{i,k}v_{i,k}\eta_{i,k}^{\gamma_1} + \sum_{k=1}^{j} r_{i,k}v_{i,k}\left|\eta_{i,k}\right|^{\gamma_2} sign(\eta_{i,k}) \\ &+ \sum_{k=1}^{j} l_{i,k}v_{i,k}sign(\eta_{i,k}) + \sum_{k=1}^{j} g_{i,k}\eta_{i,k}(x_{i,k+1}^c - \alpha_{i,k}) \\ &+ \sum_{k=1}^{j} a_{i,k,2}x_{z,i,k}\tilde{\varepsilon}_{i,k} + \sum_{k=1}^{j} \frac{\vartheta_{i,k}}{a_{i,k,1}}\tilde{W}_{i,k}^T\hat{W}_{i,k} \\ &+ \sum_{k=1}^{j} \tilde{\varepsilon}_{i,k}\dot{\varepsilon}_{i,k} + g_{i,j}v_{i,j}v_{i,j+1} + g_{i,j}\eta_{i,j}\eta_{i,j+1} \end{aligned} \tag{23}$$

Step i, n_i $(1 \le i \le n)$:

From (2) and (3), one obtains

$$\dot{x}_{i,n_i} = f_{i,n_i} + g_{i,n_i}u_i + \mu_{i,n_i} = g_{i,n_i}u_i + W_{i,n_i}^T S_{i,n_i} + \varepsilon_{i,n_i} \tag{24}$$

where $f_{i,n_i} = W_{i,n_i}^T S_{i,n_i} + \delta_{i,n_i}$, $\varepsilon_{i,n_i} = d_{i,n_i} + \delta_{i,n_i}$. There exist positive numbers $\zeta_{i,n_i,1}$ and $\zeta_{i,n_i,2}$ such that $|\varepsilon_{i,n_i}| \le |d_{i,n_i}| + |\delta_{i,n_i}| \le \zeta_{i,n_i,1}$ and $|\dot{\varepsilon}_{i,n_i}| \le |\dot{d}_{i,n_i}| + |\dot{\delta}_{i,n_i}| \le \zeta_{i,n_i,2}$ hold.

With the help of (3), (15) and (24), the derivative of z_{i,n_i} is calculated as

$$\begin{aligned}\dot{z}_{i,n_i} = &-\frac{l_{i,n_i}}{2}v_{i,n_i} - p_{i,n_i}v_{i,n_i}^{\gamma_1} - h_{i,n_i}|v_{i,n_i}|^{\gamma_2} sign(v_{i,n_i}) \\ &- g_{i,n_i-1}z_{i,n_i-1} + \tilde{W}_{i,n_i}^T S_{i,n_i} + \tilde{\varepsilon}_{i,n_i}\end{aligned} \tag{25}$$

where $\tilde{W}_{i,n_i} = W_{i,n_i} - \hat{W}_{i,n_i}$ and $\tilde{\varepsilon}_{i,n_i} = \varepsilon_{i,n_i} - \hat{\varepsilon}_{i,n_i}$ are estimation errors.

Choose the following Lyapunov function:

$$V_{i,n_i} = \sum_{k=1}^{n_i}\frac{v_{i,k}^2}{2} + \sum_{k=1}^{n_i}\frac{\eta_{i,k}^2}{2} + \sum_{k=1}^{n_i}\frac{a_{i,k,2}x_{z,i,k}^2}{2} + \sum_{k=1}^{n_i}\frac{\tilde{W}_{i,k}^T\tilde{W}_{i,k}}{2a_{i,k,1}} + \sum_{k=1}^{n_i}\frac{\tilde{\varepsilon}_{i,k}^2}{2} \tag{26}$$

Based on (10)-(12), (14) and (25), the derivative of V_{i,n_i} can be deduced as

$$\begin{aligned}\dot{V}_{i,n_i} = &-\frac{1}{2}\sum_{k=1}^{n_i}l_{i,k}v_{i,k}^2 - \sum_{k=1}^{n_i}p_{i,k}v_{i,k}^{\gamma_1+1} - \sum_{k=1}^{n_i}h_{i,k}|v_{i,k}|^{\gamma_2+1} - \sum_{k=1}^{n_i}s_{i,k}\eta_{i,k}^{\gamma_1+1} \\ &- \sum_{k=1}^{n_i}r_{i,k}|\eta_{i,k}|^{\gamma_2+1} - \sum_{k=1}^{n_i}l_{i,k}|\eta_{i,k}| - \sum_{k=1}^{n_i}\rho_{i,k,1}a_{i,k,2}x_{z,i,k}^{\gamma_1+1} \\ &- \sum_{k=1}^{n_i}\rho_{i,k,2}a_{i,k,2}|x_{z,i,k}|^{\gamma_2+1} - \sum_{k=1}^{n_i}L_{i,k}\tilde{\varepsilon}_{i,k}\tilde{W}_{i,k}^T S_{i,k} - \sum_{k=1}^{n_i}L_{i,k}\tilde{\varepsilon}_{i,k}^2 \\ &+ \sum_{k=1}^{n_i}\tilde{\varepsilon}_{i,k}\dot{\varepsilon}_{i,k} + \sum_{k=1}^{n_i}s_{i,k}v_{i,k}\eta_{i,k}^{\gamma_1} + \sum_{k=1}^{n_i}r_{i,k}v_{i,k}|\eta_{i,k}|^{\gamma_2} sign(\eta_{i,k}) \\ &+ \sum_{k=1}^{n_i}l_{i,k}v_{i,k}sign(\eta_{i,k}) + \sum_{k=1}^{n_i-1}g_{i,k}\eta_{i,k}(x_{i,k+1}^c - \alpha_{i,k}) \\ &+ \sum_{k=1}^{n_i}a_{i,k,2}x_{z,i,k}\tilde{\varepsilon}_{i,k} + \sum_{k=1}^{n_i}\frac{\vartheta_{i,k}}{a_{i,k,1}}\tilde{W}_{i,k}^T\hat{W}_{i,k}\end{aligned} \tag{27}$$

Using Young's inequality, one obtains

$$\tilde{W}_{i,k}^T\hat{W}_{i,k} \le -\frac{1}{2}\tilde{W}_{i,k}^T\tilde{W}_{i,k} + \frac{1}{2}\|W_{i,k}\|^2 \tag{28}$$

$$l_{i,k}v_{i,k}sign(\eta_{i,k}) \le \frac{l_{i,k}}{2}v_{i,k}^2 + \frac{l_{i,k}}{2}[sign(\eta_{i,k})]^2 \le \frac{l_{i,k}}{2}v_{i,k}^2 + \frac{l_{i,k}}{2} \tag{29}$$

$$\tilde{\varepsilon}_{i,k}\dot{\varepsilon}_{i,k} \le \frac{1}{2}\tilde{\varepsilon}_{i,k}^2 + \frac{1}{2}\zeta_{i,k,2}^2 \tag{30}$$

$$-\tilde{\varepsilon}_{i,k}\tilde{W}_{i,k}^T S_{i,k} \le \frac{1}{2}\tilde{\varepsilon}_{i,k}^2 + \frac{1}{2}S_{i,k}^T S_{i,k}\tilde{W}_{i,k}^T\tilde{W}_{i,k} \tag{31}$$

$$x_{z,i,k}\tilde{\varepsilon}_{i,k} \le \frac{1}{2}x_{z,i,k}^2 + \frac{1}{2}\tilde{\varepsilon}_{i,k}^2 \le \frac{1}{2}\left(x_{z,i,k}^2\right)^{\frac{1+\gamma_1}{2}} + \frac{1}{2}\left(x_{z,i,k}^2\right)^{\frac{1+\gamma_2}{2}} + \frac{1}{2}\tilde{\varepsilon}_{i,k}^2 \tag{32}$$

According to Lemma 3, the following inequalities hold.

$$\begin{cases} s_{i,k}v_{i,k}\eta_{i,k}^{\gamma_1} \le s_{i,k}|v_{i,k}||\eta_{i,k}|^{\gamma_1} \le \dfrac{s_{i,k}}{1+\gamma_1}|v_{i,k}|^{1+\gamma_1} + \dfrac{s_{i,k}\gamma_1}{1+\gamma_1}|\eta_{i,k}|^{1+\gamma_1} \\ r_{i,k}v_{i,k}|\eta_{i,k}|^{\gamma_2} sign(\eta_{i,k}) \le \dfrac{r_{i,k}}{1+\gamma_2}|v_{i,k}|^{1+\gamma_2} + \dfrac{r_{i,k}\gamma_2}{1+\gamma_2}|\eta_{i,k}|^{1+\gamma_2} \end{cases} \tag{33}$$

With the help of Assumption 2, it can be deduced that

$$\begin{aligned}g_{i,k}\eta_{i,k}\Psi_{i,k} &\le |g_{i,k}||\eta_{i,k}||\Psi_{i,k}| \le \bar{g}_2|\eta_{i,k}|\Sigma_k \le \frac{1}{2}\eta_{i,k}^2 + \frac{1}{2}\bar{g}_2^2\Sigma_k^2 \\ &\le \frac{1}{2}\left(\eta_{i,k}^2\right)^{\frac{1+\gamma_1}{2}} + \frac{1}{2}\left(\eta_{i,k}^2\right)^{\frac{1+\gamma_2}{2}} + \frac{1}{2}\bar{g}_2^2\Sigma_k^2\end{aligned} \tag{34}$$

Substituting (28)-(34) into (27), $\dot{V}_{i,n_i}$ can be rewritten as

$$\begin{aligned}\dot{V}_{i,n_i} \le &-P_1\cdot\sum_{k=1}^{n_i}\left[\left(\frac{v_{i,k}^2}{2}\right)^{\lambda_1} + \left(\frac{\eta_{i,k}^2}{2}\right)^{\lambda_1} + \left(\frac{a_{i,k,2}x_{z,i,k}^2}{2}\right)^{\lambda_1}\right] \\ &- P_2\cdot\sum_{k=1}^{n_i}\left[\left(\frac{v_{i,k}^2}{2}\right)^{\lambda_2} + \left(\frac{\eta_{i,k}^2}{2}\right)^{\lambda_2} + \left(\frac{a_{i,k,2}x_{z,i,k}^2}{2}\right)^{\lambda_2}\right] \\ &- P_1\sum_{k=1}^{n_i}\left(\frac{\tilde{W}_{i,k}^T\tilde{W}_{i,k}}{2a_{i,k,1}} + \frac{\tilde{\varepsilon}_{i,k}^2}{2}\right)^{\lambda_1} - P_2\cdot\sum_{k=1}^{n_i}\left(\frac{\tilde{W}_{i,k}^T\tilde{W}_{i,k}}{2a_{i,k,1}} + \frac{\tilde{\varepsilon}_{i,k}^2}{2}\right)^{\lambda_2} \\ &+ P_1\cdot\sum_{k=1}^{n_i}\left(\frac{\tilde{W}_{i,k}^T\tilde{W}_{i,k}}{2a_{i,k,1}} + \frac{\tilde{\varepsilon}_{i,k}^2}{2}\right)^{\lambda_1} + P_2\cdot\sum_{k=1}^{n_i}\left(\frac{\tilde{W}_{i,k}^T\tilde{W}_{i,k}}{2a_{i,k,1}} + \frac{\tilde{\varepsilon}_{i,k}^2}{2}\right)^{\lambda_2} \\ &- \sum_{k=1}^{n_i}\left(\vartheta_{i,k} - a_{i,k,1}S_{i,k}^T S_{i,k}\right)\frac{\tilde{W}_{i,k}^T\tilde{W}_{i,k}}{2a_{i,k,1}} \\ &- \sum_{k=1}^{n_i}\left(2L_{i,k} - a_{i,k,2} - 2\right)\frac{\tilde{\varepsilon}_{i,k}^2}{2} + C_{1i}\end{aligned} \tag{35}$$

where $P_1 = 2^{\lambda_1}\min\left\{p_{i,k} - s_{i,k}/(2\lambda_1), (s_{i,k} - \lambda_1)/(2\lambda_1), a_{i,k2}^{1-\lambda_1}(\rho_{i,k,1} - 0.5)\right\}$, $P_2 = 2^{\lambda_2}\min\left\{h_{i,k} - r_{i,k}/(2\lambda_2), (r_{i,k} - \lambda_2)/(2\lambda_2), a_{i,k2}^{1-\lambda_2}(\rho_{i,k,2} - 0.5)\right\}$, $\lambda_1 = (\gamma_1 + 1)/2$ and $\lambda_2 = (\gamma_2 + 1)/2$ are positive numbers, $C_{1i} = 0.5\sum_{k=1}^{n_i}(l_{i,k} + \zeta_{i,k,2}^2) + 0.5\sum_{k=1}^{n_i}\left(\vartheta_{i,k}\|W_{i,k}\|^2/a_{i,k,1} + \bar{g}_2^2\Sigma_k^2\right)$.

According to Lemma 2, Eq. (35) can be converted as

$$\begin{aligned}\dot{V}_{i,n_i} \le &-P_1\cdot n_i^{1-\lambda_1}V_{i,n_i}^{\lambda_1} - P_2\cdot V_{i,n_i}^{\lambda_2} \\ &+ P_1\cdot\sum_{k=1}^{n_i}\left(\frac{\tilde{W}_{i,k}^T\tilde{W}_{i,k}}{2a_{i,k,1}} + \frac{\tilde{\varepsilon}_{i,k}^2}{2}\right)^{\lambda_1} + P_2\cdot\sum_{k=1}^{n_i}\left(\frac{\tilde{W}_{i,k}^T\tilde{W}_{i,k}}{2a_{i,k,1}} + \frac{\tilde{\varepsilon}_{i,k}^2}{2}\right)^{\lambda_2} \\ &- \sum_{k=1}^{n_i}\left(\vartheta_{i,k} - a_{i,k,1}S_{i,k}^T S_{i,k}\right)\frac{\tilde{W}_{i,k}^T\tilde{W}_{i,k}}{2a_{i,k,1}} \\ &- \sum_{k=1}^{n_i}\left(2L_{i,k} - a_{i,k,2} - 2\right)\frac{\tilde{\varepsilon}_{i,k}^2}{2} + C_{1i}\end{aligned} \tag{36}$$

Based on Lemma 3, define $x = 1$, $y = \tilde{W}_{i,k}^T\tilde{W}_{i,k}/(2a_{i,k,1}) + \tilde{\varepsilon}_{i,k}^2/2$, $p = 1 - \lambda_2 > 0$, $q = \lambda_2 > 0$ and $s = \lambda_2^{\lambda_2/(1-\lambda_2)}$, the following is obtained.

$$\left(\frac{\tilde{W}_{i,k}^T\tilde{W}_{i,k}}{2a_{i,k,1}} + \frac{\tilde{\varepsilon}_{i,k}^2}{2}\right)^{\lambda_2} \le (1-\lambda_2)\lambda_2^{\lambda_2/(1-\lambda_2)} + \frac{\tilde{W}_{i,k}^T\tilde{W}_{i,k}}{2a_{i,k,1}} + \frac{\tilde{\varepsilon}_{i,k}^2}{2} \tag{37}$$

Suppose there is a unknown constant $\omega_{i,k} > 0$ such that $\tilde{W}_{i,k}^T\tilde{W}_{i,k}/(2a_{i,k,1}) + \tilde{\varepsilon}_{i,k}^2/2 \le \omega_{i,k}$ holds, then

If $\tilde{W}_{i,k}^T\tilde{W}_{i,k}/(2a_{i,k,1}) + \tilde{\varepsilon}_{i,k}^2/2 \le 1$, one obtains

$$\left(\frac{\tilde{W}_{i,k}^T\tilde{W}_{i,k}}{2a_{i,k,1}}+\frac{\tilde{\varepsilon}_{i,k}^2}{2}\right)^{\lambda_1}\le 1 \tag{38}$$

If $\tilde{W}_{i,k}^T\tilde{W}_{i,k}/(2a_{i,k,1})+\tilde{\varepsilon}_{i,k}^2/2>1$, it can be seen that

$$\left(\frac{\tilde{W}_{i,k}^T\tilde{W}_{i,k}}{2a_{i,k,1}}+\frac{\tilde{\varepsilon}_{i,k}^2}{2}\right)^{\lambda_1}\le \omega_{i,k}^{\lambda_1} \tag{39}$$

According to (38) and (39), the following inequality holds.

$$\left(\frac{\tilde{W}_{i,k}^T\tilde{W}_{i,k}}{2a_{i,k,1}}+\frac{\tilde{\varepsilon}_{i,k}^2}{2}\right)^{\lambda_1}\le \omega_{i,k}^{\lambda_1}+1 \tag{40}$$

Substitute (37) and (40) into (36), $\dot{V}_{i,n_i}$ can be deduced as

$$\dot{V}_{i,n_i}\le -P_1\cdot n_i^{1-\lambda_1}V_{i,n_i}^{\lambda_1}-P_2\cdot V_{i,n_i}^{\lambda_2}+C_{2i} \tag{41}$$

where $\vartheta_{i,k}-a_{i,k,1}S_{i,k}^TS_{i,k}-P_2>0$ and $2L_{i,k}-P_2-a_{i,k,2}-2>0$ hold, $C_{2i}=C_{1i}+P_1\sum_{k=1}^{n_i}(\omega_{i,k}^{\lambda_1}+1)+P_2n_i(1-\lambda_2)\lambda_2^{\lambda_2/(1-\lambda_2)}$.

The total Lyapunov function is designed as $V=\sum_{i=1}^{n}V_{i,n_i}$, it can be deduced that

$$\dot{V}\le -H_1V^{\lambda_1}-H_2V^{\lambda_2}+C \tag{42}$$

where $H_1=n^{1-\lambda_1}\min\{P_1n_i^{1-\lambda_1}\}$, $H_2=\min\{P_2\}$ and $C=\sum_{i=1}^{n}C_{2i}$.

The Lemma 1 can be satisfied if appropriate parameters are selected such that $H_1>0$, $H_2>0$ and $0<C<\infty$ hold. The control plant (2) is practically FiTS and the settling time is given by

$$T\le T_{\max}=\frac{1}{H_1\bar{\varsigma}(\lambda_1-1)}+\frac{1}{H_2\bar{\varsigma}(1-\lambda_2)} \tag{43}$$

All signals of the control system converge to the following compact set:

$$x\in\min\left\{V(x)\le\left(\frac{C}{(1-\bar{\varsigma})H_1}\right)^{\frac{1}{\lambda_1}},\left(\frac{C}{(1-\bar{\varsigma})H_2}\right)^{\frac{1}{\lambda_2}}\right\} \tag{44}$$

where $0<\bar{\varsigma}<1$.

Through above analysis, it can be seen that $v_{i,j}$, $\eta_{i,j}$, $x_{z,i,j}$, $\tilde{W}_{i,j}$ and $\tilde{\varepsilon}_{i,j}$ are bounded, $j=1,2,...,n_i$, $i=1,2,...,n$. Thus, $\hat{W}_{i,j}$ and $\hat{\varepsilon}_{i,j}$ are also bounded. In view of these results, it is easy to deduce that all signals of the control plant are bounded and the tracking error will converge to a small neighborhood of the origin within a fixed time.

The proof is completed.

Remark 3. Compared with previous studies, the main contributions of presented control scheme are two-fold. Firstly, approximation performances of NNs are promoted by utilizing prediction errors and compensation signals to construct NAL. Different from the existing methods (Xu et al., 2020; Xu and Sun, 2018; Sun et al., 2020; Xu, 2018; Wang et al., 2018b; Li et al., 2015; Sun et al., 2022), the prediction errors are derived from the novel SPEM (11). Secondly, the ADOs (13) and (14) are designed to estimate lumped disturbances. Based on CFB design framework, the virtual controller (6), (7) and FECSs (8)-(10) are constructed to ensure that the control system is stable in a fixed time.

Remark 4. The parameter values of the proposed control method are usually selected according to the characteristics of the control plant and the condition that meet the stability standard. That is, all parameters need to satisfy Theorem 1. Specifically, $\vartheta_{i,k}-a_{i,k,1}S_{i,k}^TS_{i,k}-P_2>0$, $2L_{i,k}-P_2-a_{i,k,2}-2>0$, $H_1=n^{1-\lambda_1}\min\{P_1n_i^{1-\lambda_1}\}>0$, $H_2=\min\{P_2\}>0$ and $C=\sum_{i=1}^{n}C_{2i}>0$ should be ensured. Based on (35) and (41), it can be seen that $P_1=2^{\lambda_1}\min\left\{p_{i,k}-s_{i,k}/(2\lambda_1),(s_{i,k}-\lambda_1)/(2\lambda_1),a_{i,k,2}^{1-\lambda_1}(\rho_{i,k,1}-0.5)\right\}$, $P_2=2^{\lambda_2}\min\left\{h_{i,k}-r_{i,k}/(2\lambda_2),(r_{i,k}-\lambda_2)/(2\lambda_2),a_{i,k,2}^{1-\lambda_2}(\rho_{i,k,2}-0.5)\right\}$ and $C_{2i}=C_{1i}+P_1\sum_{k=1}^{n_i}(\omega_{i,k}^{\lambda_1}+1)+P_2n_i(1-\lambda_2)\lambda_2^{\lambda_2/(1-\lambda_2)}$. Obviously, $C_{2i}>0$ hold. In order to make $P_1>0$, $p_{i,k}-s_{i,k}/(2\lambda_1)>0$, $(s_{i,k}-\lambda_1)/(2\lambda_1)>0$ and $a_{i,k2}^{1-\lambda_1}(\rho_{i,k,1}-0.5)>0$ should be guaranteed. Similarly, $h_{i,k}-r_{i,k}/(2\lambda_2)>0$, $(r_{i,k}-\lambda_2)/(2\lambda_2)>0$ and $a_{i,k2}^{1-\lambda_2}(\rho_{i,k,2}-0.5)>0$ should be satisfied to ensure $P_2>0$, $k=1,2,...,n_i$, $i=1,2,...,n$. According to (43), the convergence rate can be improved by increasing H_1 and H_2. In order to increase H_1, the large $p_{i,k}$, $s_{i,k}$ and $\rho_{i,k,1}$ should be selected. Particularly, $p_{i,k}$ should be selected as large as possible to compensate large $s_{i,k}$. Choose large $h_{i,k}$, $r_{i,k}$ and $\rho_{i,k,2}$ to increase H_2, and $h_{i,k}$ is selected as large as possible to compensate large $r_{i,k}$. The selection of $a_{i,k,2}$ is complicated due to $\lambda_1>1$ and $\lambda_2<1$. A large $a_{i,k,2}$ will cause small $a_{i,k,2}^{1-\lambda_1}$ and large $a_{i,k,2}^{1-\lambda_2}$, while a small $a_{i,k,2}$ will cause large $a_{i,k,2}^{1-\lambda_1}$ and small $a_{i,k,2}^{1-\lambda_2}$. The selection of $a_{i,k,2}$ needs to be adjusted according to the actual situation. In addition, too large control parameters may result in the input saturation. Therefore, when selecting control parameters, it is necessary to keep a balance between the system stability and the control effect.

4. SIMULATION RESULTS

In this part, two representative examples are presented to show the superiority of the designed control method.

Example 1. The dynamic model of the exoskeleton system can be expressed as (Song et al., 2018)

$$\begin{aligned}\dot{x}_1&=x_2\\ \dot{x}_2&=M^{-1}(x_1)\left[\tau-d-f-G(x_1)-C(x_1,x_2)x_2\right]\\ y&=x_1\end{aligned} \tag{45}$$

where $x_1=[x_{11},x_{12}]^T$, $x_2=[x_{21},x_{22}]^T$ and $\dot{x}_2=[\dot{x}_{21},\dot{x}_{22}]^T$ represent the joint angle, angle velocity and angle acceleration, respectively. The definitions of $M(x_1)$, $C(x_1,x_2)$, $G(x_1)$ and their values are given in (Song et al., 2018), $f=[f_1,f_2]^T$ stands for model uncertainty, $d=[d_1,d_2]^T$ represents external disturbance, $\tau=[\tau_1,\tau_2]^T$ represents the input torque, $y=[y_1,y_2]^T$ denotes the output angle.

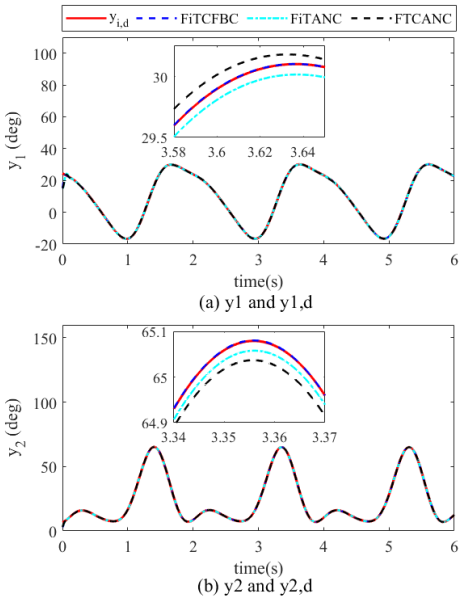

Fig. 1. The trajectories of output angle yi and desired angle yi,d.

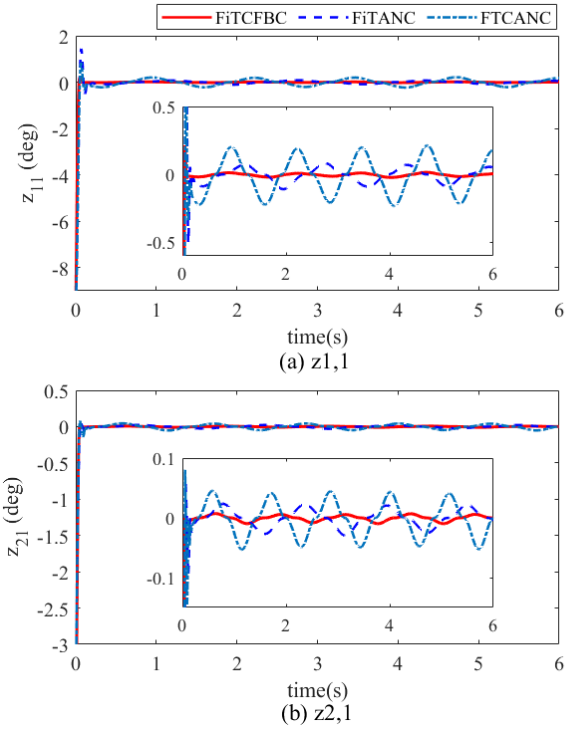

Fig. 2. The trajectories of tracking errors $z_{i,1}$.

$\tau=[\tau_1,\tau_2]^T$ represents the input torque, $y=[y_1,y_2]^T$ denotes the output angle.

Control parameters are chosen as $\gamma_1=3$, $\gamma_2=0.6$, $k_{i,1,1}=k_{i,1,3}=30$, $k_{i,1,2}=k_{i,1,4}=25$, $l_{i,1,1}=l_{i,1,3}=2$, $l_{i,1,2}=l_{i,1,4}=0.5$, $p_{i,1}=20$, $p_{i,2}=18$, $h_{i,1}=25$, $h_{i,2}=20$, $s_{i,1}=s_{i,2}=15$, $r_{i,1}=r_{i,2}=8$, $l_{i,1}=8$, $l_{i,2}=6$, $\rho_{i,1,1}=\rho_{i,2,1}=15$, $\rho_{i,1,2}=\rho_{i,2,2}=18$, $a_{i,1,1}=a_{i,2,1}=5$, $a_{i,1,2}=a_{i,2,2}=8$, $\vartheta_{i,1}=\vartheta_{i,2}=15$, $L_{i,1}=L_{i,2}=12$, $i=1,2$.

Initial conditions are set as $[x_{11}(0),x_{12}(0),x_{21}(0),x_{22}(0)]^T=[15,3,0,0]^T$. External disturbances are chosen as $d_1=4\sin(4t)$ and $d_2=4\cos(4t)$. The input of the RBFNN is $Z_{i,2}=[x_{i,1}^T,x_{i,2}^T,x_{i,2}^c,v_{i,1}^T,v_{i,2}^T]$, $i=1,2$, the node number is 256. The width parameters of the basis function are all designed to be 10, and network centers are all evenly distributed in $[-1,1]$.

This example is to verify the effectiveness of the proposed control approach (FiTCFBC) by compared with FiTANC (Ba et al., 2019) and FTCANC (Sun et al., 2022).

For the fair comparison, the design parameters of these methods are identical. Figs. 1 and 2 depict contrastive results. The tracking performances of these methods are shown in Fig. 1, and Fig. 2 portrays tracking errors. Although tracking performances are all achieved, the tracking error $z_{i,1}$ in this paper is smaller than those two methods. It can be clearly seen that the designed FiTCFBC is better than FiTANC and FTCANC in tracking effect.

In order to assess the system performance, integral absolute error (IAE) and integral time absolute error (ITAE) are introduced as performance indicators to quantify tracking errors. When these indicators are smaller, the control performance is better.

IAE and ITAE are defined as

$$\begin{cases} IAE(z_{i,1})=\int_{t_0}^{t_f}|z_{i,1}|dt \\ ITAE(z_{i,1})=\int_{t_0}^{t_f}t|z_{i,1}|dt \end{cases} \tag{46}$$

where $t_0=0$ and $t_f=6$ are the starting and ending moments respectively.

Table 1 expresses performance indicators and the comparison results are shown in Fig. 3. These results obviously show that FiTCFBC is better than FiTANC and FTCANC in trajectory tracking.

Table 1. Performance indicators.

Methods	IAE(z_{11})	IAE(z_{21})	ITAE(z_{11})	ITAE(z_{21})
FiTCFBC	0.2211	0.1004	0.1572	0.0661
FiTANC	0.5660	0.1476	0.7264	0.1983
FTCANC	0.9331	0.2111	1.9626	0.4197

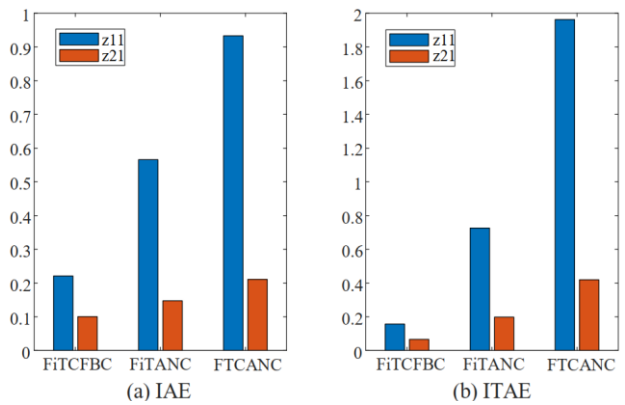

Fig. 3. Comparisons for performance indicators.

Example 2. Consider the following MIMO nonlinear system with external disturbances (Yu et al., 2020):

$$\begin{cases} \dot{x}_{1,1} = x_{1,2} \\ \dot{x}_{1,2} = f_{1,2}(\bar{x}_{1,2}) + g_{1,2}(\bar{x}_{1,2})u_1 + d_{1,2} \\ y_1 = x_{1,1} \end{cases} \tag{47}$$

$$\begin{cases} \dot{x}_{2,1} = x_{2,2} \\ \dot{x}_{2,2} = f_{2,2}(\bar{x}_{2,2}) + g_{2,2}(\bar{x}_{1,2})u_2 + d_{2,2} \\ y_2 = x_{2,1} \end{cases} \tag{48}$$

where external disturbances are chosen as $d_{1,2} = 6\sin(5t)$ and $d_{2,2} = 6\cos(5t)$. Control gains are chosen as $g_{1,2} = 2$ and $g_{2,2} = 5$. $f_{1,2}$ and $f_{2,2}$ are unknown nonlinear functions.

Desired signals are $y_{1,d} = 2.5\sin(t) + 3\cos(0.5t) - 2$ and $y_{2,d} = 2\sin(0.5t) - \cos(t) + 3$. Initial values are set as 0. The input of RBFNN is $Z_{i,j} = \bar{x}_{i,j} = [x_{i,1}, x_{i,2}]^T$, $i = 1,2$, the nodes of hidden layer are 32. The width parameters are all designed as 0.8, network centers are evenly distributed in $[-9, 9]$.

Control parameters are chosen as $\gamma_1 = 3$, $\gamma_2 = 0.6$, $k_{i,1,1} = k_{i,1,3} = 22$, $k_{i,1,2} = k_{i,1,4} = 20$, $l_{i,1,1} = l_{i,1,3} = 1.2$, $l_{i,1,2} = l_{i,1,4} = 0.3$, $p_{i,1} = 10$, $p_{i,2} = 12$, $h_{i,1} = 15$, $h_{i,2} = 10$, $s_{i,1} = s_{i,2} = 10$, $r_{i,1} = r_{i,2} = 5$, $l_{i,1} = 5$, $l_{i,2} = 4$, $\rho_{i,1,1} = \rho_{i,2,1} = 5$, $\rho_{i,1,2} = \rho_{i,2,2} = 6$, $a_{i,1,1} = a_{i,2,1} = 2$, $a_{i,1,2} = a_{i,2,2} = 2$, $\vartheta_{i,1} = \vartheta_{i,2} = 10$, $L_{i,1} = 5.4$, $L_{i,2} = 6.2$, $i = 1,2$.

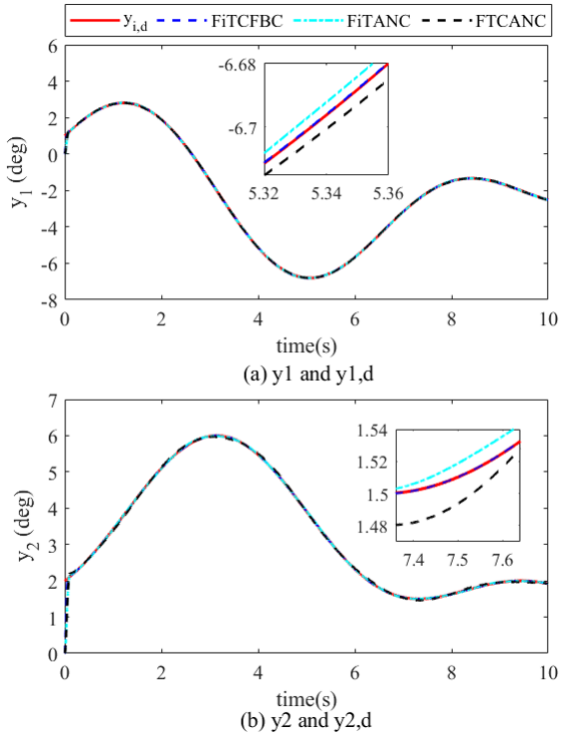

Fig. 4. The trajectories of yi and yi,d.

Similar to Example 1, FiTCFBC, FiTANC and FTCANC are compared in tracking precision. Select same control parameters to ensure the impartial comparison. Fig. 4 illustrates tracking results of these control methods. Tracking errors are depicted in Fig. 5. One can reach the consistent conclusion that the proposed FiTCFBC has higher tracking accuracy than FiTANC and FTCANC.

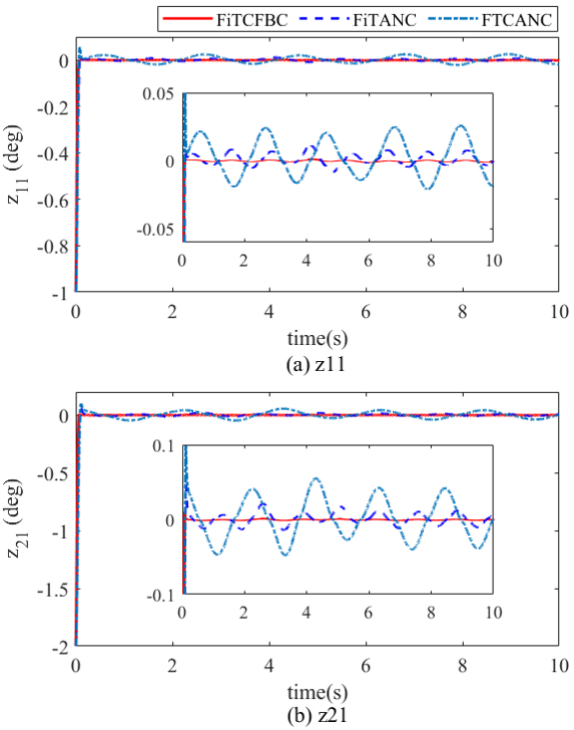

Fig. 5. The trajectories of $z_{i,1}$.

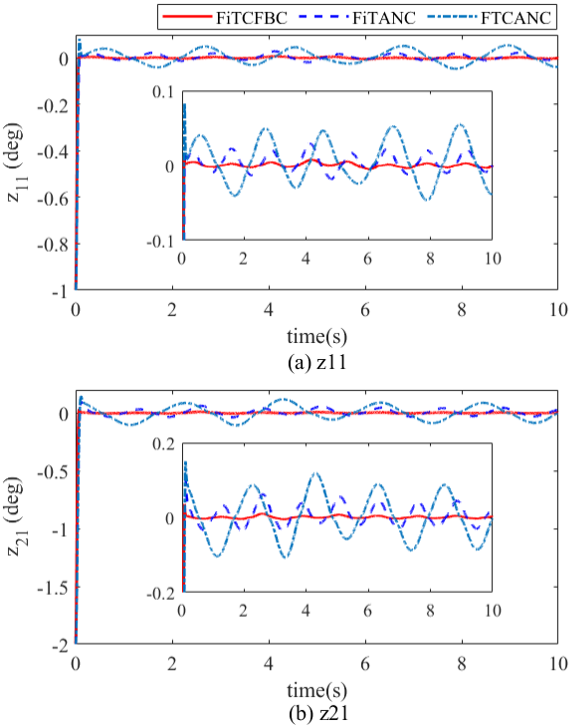

Fig. 6. The trajectories of $z_{i,1}$ for larger disturbances.

Moreover, there are two methods to test the robustness of the control scheme. One is the variation of dynamic parameters and external disturbances. The other is the influence of controller parameters on system performance. $IAE[(z_{11} + z_{21})/2]$

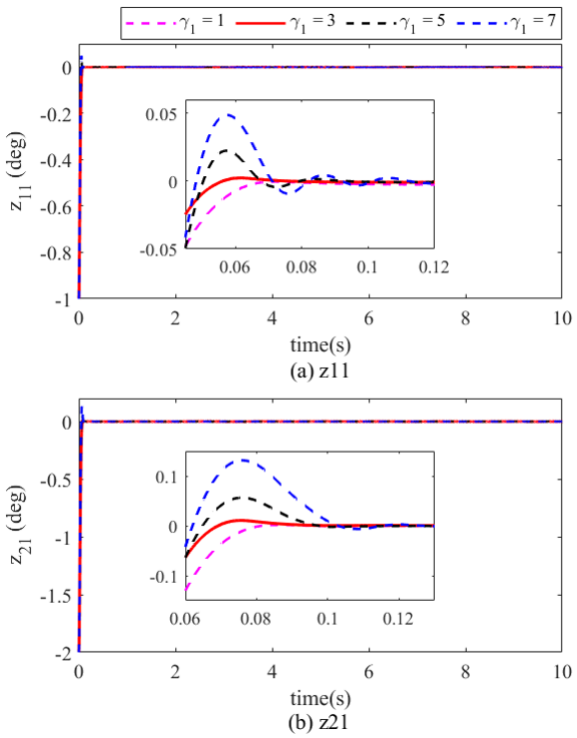

Fig. 7. The trajectories of $z_{i,1}$ for different γ_1.

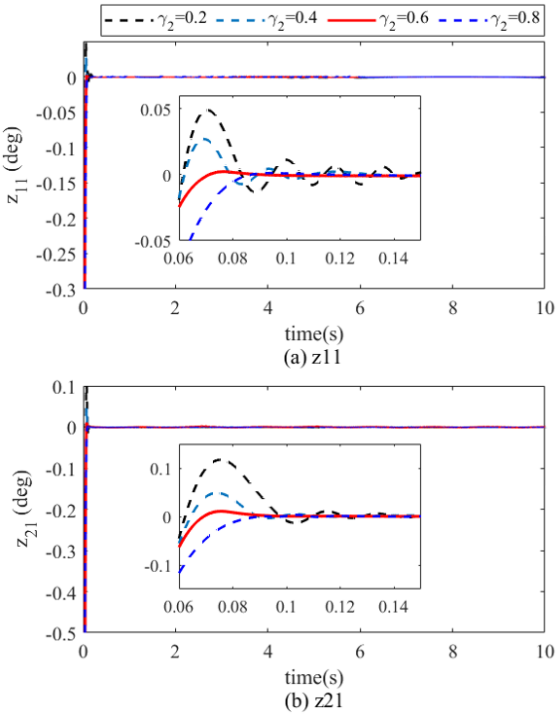

Fig. 8. The trajectories of $z_{i,1}$ for different γ_2.

is used as a performance indicator to quantify the control effect. The robustness is verified by following Cases.

Case 1. The changes in dynamic parameters and external disturbances.

Compared with the initial conditions, the dynamic parameters in (47) and (48) are increased 50%, that is $f_{1,2}=1.5x_{11}\sin(x_{21})+3$, $f_{2,2}=3x_{21}\cos(x_{11})+3$, $g_{1,2}=3$ and $g_{2,2}=7.5$. The external disturbances are chosen as $d_{1,2}=12\sin(5t)$ and $d_{2,2}=12\cos(5t)$. Simulation results for tracking errors are portrayed in Fig. 6. It is noteworthy that developed FiTCFBC still realize desired tracking precision.

In Fig. 5, $IAE(FiCFBC)=0.0472$, $IAE(FiTANC)=0.1048$ and $IAE(FTCANC)=0.2131$ can be calculated. In Fig. 6, it can be obtained that $IAE(FiCFBC)=0.0523$, $IAE(FiTANC)=0.1185$ and $IAE(FTCANC)=0.2419$. Hence, the performances of FiTCFBC, FiTANC and FTCANC decrease by 10.81%, 13.07% and 13.51% respectively. Obviously, the FiTCFBC is more robust than those two methods.

Case 2. Parameter variations of the controller.

Because there are many parameters, the constants γ_1, γ_2 and $h_{i,1}$ are as examples. Firstly, all parameters are fixed but γ_1 takes different values, such as 1, 3, 5 and 7. Fig. 7 demonstrates the results.

As can be seen from Fig. 7, although γ_1 takes different values, it can ensure that tracking errors converge to the neighborhood of the origin within a fixed time. When $\gamma_1>3$, the overshoot of tracking error will enlarge with the increase of γ_1. With the help of performance indicator $IAE[(z_{11}+z_{21})/2]$, the indicators corresponding to γ_1=1, γ_1=3, γ_1=5 and γ_1=7 are 0.0511, 0.0472, 0.0523 and 0.0532, respectively. Compared with γ_1=3, the system performances of γ_1=1, γ_1=5 and γ_1=7 degrade by 8.26%, 10.81% and 12.71%, respectively. Thus, $\gamma_1=3$ is the final selection.

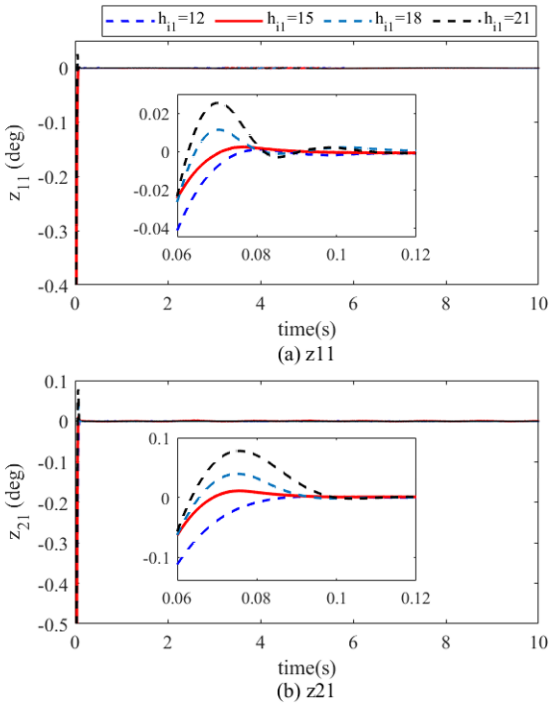

Fig. 9. The trajectories of $z_{i,1}$ for different $h_{i,1}$.

Secondly, all parameters are fixed but γ_2 takes different values, such as 0.2, 0.4, 0.6 and 0.8. The comparison results are illustrated in Fig. 8.

From Fig. 8, the tracking errors still realize convergence in a fixed time regardless of different γ_2. When $0<\gamma_2<0.6$, the overshoot of tracking error will enlarge with the decrease of γ_2. There is a small oscillation if $\gamma_2=0.2$. Specifically, the performance indicators for $\gamma_2=0.2$, $\gamma_2=0.4$, $\gamma_2=0.6$ and $\gamma_2=0.8$ are 0.0539, 0.0528, 0.0472 and 0.0517, respectively. Compared with $\gamma_2=0.6$, the system performances of $\gamma_2=0.2$, $\gamma_2=0.4$ and $\gamma_2=0.8$ decrease by 14.19%, 11.86% and 9.53%, respectively. Hence, $\gamma_2=0.6$ is the final value.

Thirdly, all parameters are fixed but $h_{i,1}$ takes different values, such as 12, 15, 18 and 21. Fig. 9 shows comparison results.

According to Fig. 9, the fixed-time convergence for tracking error is also achieved. When $h_{i,1}>15$, with the increase of $h_{i,1}$, the overshoot of tracking error is also increasing. The performance indicators about $h_{i,1}=12$, $h_{i,1}=15$, $h_{i,1}=18$ and $h_{i,1}=21$ are 0.0501, 0.0472, 0.0491 and 0.0504, respectively. Compared with $h_{i,1}=15$, the system performances of $h_{i,1}=12$, $h_{i,1}=18$ and $h_{i,1}=21$ degrade by 6.14%, 4.03% and 6.78%, respectively. Then $h_{i,1}=15$ is a satisfactory choice.

Based on above analysis, the tracking errors always converge to the neighborhood near the origin in a fixed time. The control parameters selected in this paper are reasonable and the designed control method is robust.

5. CONCLUSIONS

In this paper, a CFB-based fixed-time adaptive control algorithm is designed to address the tracking problem for uncertain MIMO nonlinear systems with external disturbances. Firstly, the tracking errors can converge to the small vicinity of origin within a fixed time through designing new virtual controllers and FECSs. All signals of control system are bounded and the settling time is only related to control parameters. Secondly, by structuring prediction errors from SPEMs, the NALs are synthesized by prediction errors and error compensation signals to improve approximation capacities. Thirdly, the presented ADOs are utilized to estimate lumped disturbances to improve control performance. Finally, the simulation results verify the effectiveness of the proposed control method. The future research direction will focus on reducing control parameters to decrease the computational burden and studying fixed-time control with specified performance.

REFERENCES

Ata, B. and Coban, R. (2022). Decoupled adaptive backstepping sliding mode control of underactuated mechanical systems. Journal of Control Engineering and Applied Informatics, 24(1), 45–56.

Ba, D., Li, Y.X., and Tong, S. (2019). Fixed-time adaptive neural tracking control for a class of uncertain nonstrict nonlinear systems. Neurocomputing, 363, 273–280.

Cao, X., Shi, P., Li, Z., and Liu, M. (2018). Neural-networkbased adaptive backstepping control with application to spacecraft attitude regulation. IEEE transactions on neural networks and learning systems, 29(9), 4303–4313.

Chen, B. and Lin, C. (2021). Finite-time stabilization-based adaptive fuzzy control design. IEEE Transactions on Fuzzy Systems, 29(8), 2438–2443.

Chen, M., Ge, S.S., and How, B.V.E. (2010). Robust adaptive neural network control for a class of uncertain mimo nonlinear systems with input nonlinearities. IEEE Transactions on Neural Networks, 21(5), 796–812.

Dong, H., Zhang, S., Li, B., and Yan, Q. (2022). Research on hydraulic looper system modeling and rbf neural network decoupling control. Journal of Control Engineering and Applied Informatics, 24(1), 57–67.

Dong, W., Farrell, J. A., Polycarpou, M.M., Djapic, V., and Sharma, M. (2012). Command filtered adaptive backstepping. IEEE Transactions on Control Systems Technology, 20(3), 566–580.

Euldji, R., Batel, N., Rebhi, R., and Skender, M.R. (2022). Optimal anfis-fopid with back-stepping controller design for wheeled mobile robot control. Journal of Control Engineering and Applied Informatics, 24(2), 57–68.

Farrell, J.A., Polycarpou, M., Sharma, M., and Dong, W. (2009). Command filtered backstepping. IEEE Transactions on Automatic Control, 54(6), 1391–1395.

Gao, Z. and Guo, G. (2019). Command-filtered fixed-time trajectory tracking control of surface vehicles based on a disturbance observer. International Journal of Robust and Nonlinear Control, 29(13), 4348–4365.

Guo, X., Ma, H., Liang, H., and Zhang, H. (2022). Commandfilter-based fixed-time bipartite containment control for a class of stochastic multiagent systems. IEEE Transactions on Systems, Man, and Cybernetics: Systems, 52(6), 3519–3529.

Jebri, A., Madani, T., Djouani, K., and Benallegue, A. (2020). Robust adaptive neuronal controller for exoskeletons with sliding-mode. Neurocomputing, 399, 317–330.

Kanchanaharuthai, A. and Mujjalinvimut, E. (2022). Fixedtime command-filtered backstepping control design for hydraulic turbine regulating systems. Renewable Energy, 184, 1091–1103.

Li, Y., Tong, S., and Li, T. (2015). Composite adaptive fuzzy output feedback control design for uncertain nonlinear strictfeedback systems with input saturation. IEEE Transactions on Cybernetics, 45(10), 2299–2308.

Liu, H., Pan, Y., and Cao, J. (2020). Composite learning adaptive dynamic surface control of fractional-order nonlinear systems. IEEE Transactions on Cybernetics, 50(6), 2557–2567.

Ma, H., Liang, H., Zhou, Q., and Ahn, C.K. (2019). Adaptive dynamic surface control design for uncertain nonlinear strict-feedback systems with unknown control direction and disturbances. IEEE Transactions on Systems, Man, and Cybernetics: Systems, 49(3), 506–515.

Niu, B., Liu, Y., Zong, G., Han, Z., and Fu, J. (2017). Command filter-based adaptive neural tracking controller design for uncertain switched nonlinear output-constrained systems. IEEE Transactions on Cybernetics, 47(10), 3160–3171.

Polyakov, A. (2012). Nonlinear feedback design for fixed-time stabilization of linear control systems. IEEE Transactions on Automatic Control, 57(8), 2106–2110.

Qian, C. and Lin, W. (2001). Non-lipschitz continuous stabilizers for nonlinear systems with uncontrollable unstable linearization. Systems & Control Letters, 42(3), 185–200.

Qiu, J., Sun, K., Rudas, I.J., and Gao, H. (2020). Command filter-based adaptive nn control for mimo nonlinear systems with full-state constraints and actuator hysteresis. IEEE transactions on cybernetics, 50(7), 2905–2915.

Shojaei, F., Arefi, M.M., Khayatian, A., and Karimi, H.R. (2019). Observer-based fuzzy adaptive dynamic surface control of uncertain nonstrict feedback systems with unknown control direction and unknown dead-zone. IEEE Transactions on Systems, Man, and Cybernetics: Systems, 49(11), 2340–2351.

Song, S., Cao, Y., Wang, H., Xue, J., Zhang, X., Fu, J., and Tu, F. (2018). Adaptive output feedback force tracking control for lower extremity power-assisted exoskeleton. Journal of Control Engineering and Applied Informatics, 20(3), 60–68.

Song, S., Park, J.H., Zhang, B., and Song, X. (2021). Eventtriggered adaptive practical fixed-time trajectory tracking control for unmanned surface vehicle. IEEE Transactions on Circuits and Systems II: Express Briefs, 68(1), 436–440.

Sun, J., He, H., Yi, J., and Pu, Z. (2022). Finite-time commandfiltered composite adaptive neural control of uncertain nonlinear systems. IEEE Transactions on Cybernetics, 52(7), 6809–6821.

Sun, T., Peng, L., Cheng, L., Hou, Z.G., and Pan, Y. (2020). Composite learning enhanced robot impedance control. IEEE Transactions on Neural Networks and Learning Systems, 31(3), 1052–1059.

Sun, W., Diao, S., Su, S.F., and Sun, Z.Y. (2023). Fixed-time adaptive neural network control for nonlinear systems with input saturation. IEEE Transactions on Neural Networks and Learning Systems, 34(4), 1911–1920.

Swaroop, D., Hedrick, J.K., Yip, P.P., and Gerdes, J.C. (2000). Dynamic surface control for a class of nonlinear systems. IEEE transactions on automatic control, 45(10), 1893–1899.

Vallejo-Alarcon, M.A. (2020). Robust backstepping control for highly demanding quadrotor flight. Journal of Control Engineering and Applied Informatics, 22(1), 51–62.

Van, M., Mavrovouniotis, M., and Ge, S.S. (2019). An adaptive backstepping nonsingular fast terminal sliding mode control for robust fault tolerant control of robot manipulators. IEEE Transactions on Systems, Man, and Cybernetics: Systems, 49(7), 1448–1458.

Van Tran, T. and Wang, Y. (2017). Artificial chemical reaction optimization algorithm and neural network based adaptive control for robot manipulator. Journal of Control Engineering and Applied Informatics, 19(2), 61–70.

Wang, H., Liu, P.X., Li, S., and Wang, D. (2018a). Adaptive neural output-feedback control for a class of nonlower triangular nonlinear systems with unmodeled dynamics. IEEE transactions on neural networks and learning systems, 29(8), 3658–3668.

Wang, L., Basin, M.V., Li, H., and Lu, R. (2018b). Observerbased composite adaptive fuzzy control for nonstrictfeedback systems with actuator failures. IEEE Transactions on Fuzzy Systems, 26(4), 2336–2347.

Xu, B. (2018). Composite learning control of flexible-link manipulator using nn and dob. IEEE Transactions on Systems, Man, and Cybernetics: Systems, 48(11), 1979–1985.

Xu, B. and Sun, F. (2018). Composite intelligent learning control of strict-feedback systems with disturbance. IEEE transactions on cybernetics, 48(2), 730–741.

Xu, B., Zhang, R., Li, S., He, W., and Shi, Z. (2020). Composite neural learning-based nonsingular terminal sliding mode control of mems gyroscopes. IEEE Transactions on Neural networks and learning systems, 31(4), 1375–1386.

Yang, H. and Ye, D. (2018). Adaptive fixed-time bipartite tracking consensus control for unknown nonlinear multiagent systems: An information classification mechanism. Information Sciences, 459, 238–254.

Yang, W., Pan, Y., and Liang, H. (2021). Event-triggered adaptive fixed-time nn control for constrained nonstrict-feedback nonlinear systems with prescribed performance. Neurocomputing, 422, 332–344.

Yu, J., Shi, P., Lin, C., and Yu, H. (2020). Adaptive neural command filtering control for nonlinear mimo systems with saturation input and unknown control direction. IEEE Transactions on Cybernetics, 50(6), 2536–2545.

Yu, J., Shi, P., and Zhao, L. (2018). Finite-time command filtered backstepping control for a class of nonlinear systems. Automatica, 92, 173–180.

Zhang, S., Dong, Y., Ouyang, Y., Yin, Z., and Peng, K. (2018). Adaptive neural control for robotic manipulators with output constraints and uncertainties. IEEE transactions on neural networks and learning systems, 29(11), 5554–5564.

Zhao, K. and Song, Y. (2019). Removing the feasibility conditions imposed on tracking control designs for stateconstrained strict-feedback systems. IEEE Transactions on Automatic Control, 64(3), 1265–1272.

Zuo, Z. and Tie, L. (2014). Distributed robust finite-time nonlinear consensus protocols for multi-agent systems. International Journal of Systems Science, 47(6), 1366–1375.